Estimating signal and structured noise in ultrasound data using prediction-error filters

Joseph Jennings, Marko Jakovljevic, Ettore Biondi, Jeremy Dahl, Biondo Biondi

Joseph Jennings, Marko Jakovljevic, Ettore Biondi, Jeremy Dahl, Biondo Biondi, "Estimating signal and structured noise in ultrasound data using prediction-error filters," Proc. SPIE 10955, Medical Imaging 2019: Ultrasonic Imaging and Tomography, 109550R (15 March 2019); doi: 10.1117/12.2513514

SPIE.

Event: SPIE Medical Imaging, 2019, San Diego, California, United States

Estimating Signal and Structured Noise in Ultrasound Data using Prediction-Error Filters

Joseph Jennings[1,*], Marko Jakovljevic[2,*], Ettore Biondi[1,*], Jeremy Dahl[2,+], and Biondo Biondi[1,+]

[1]Department of Geophysics, School of Earth, Energy and Environmental Sciences, Stanford University, Stanford 94305

[2]Department of Radiology, School of Medicine, Stanford University, Palo Alto, CA 94304

[*]The authors made equal contributions towards the conference submission.

[+]The authors made equal contributions towards the conference submission.

ABSTRACT

When using ultrasound to image heterogeneous media, echoes from multiple and off-axis scattering can overwrite the recorded ballistic wavefronts of interest. This reduces the coherence of signals across the aperture and causes clutter in the final image. Therefore, separating those unwanted events from the signal of interest is necessary to improve the visibility of structures in a B-mode image, and also to enable other processing methods that require coherent channel signals, such as various phase-aberration-correction techniques and sound-speed estimators.

We used prediction-error filters (PEFs) to model the signal and the assumed additive noise in the data acquired through a 10 mm thick layer of beef tissue placed above a speckle region of a phantom. The PEF coefficients used to model the signal were first computed from the phantom data collected without tissue and subsequently employed to deconvolve the tissue data and find the PEF associated with the noise. These two filters were then used in a joint-inversion framework to separate the signal and noise components recorded within the original tissue data. In order to be able to apply our method in scenarios where direct measurements of the signal proxy are not available, we also evaluated the signal-PEF coefficients from the theoretical model of the signal from diffuse targets as provided by the van-Cittert Zernike (VCZ) theorem.

To evaluate the quality of the separation of signal from the noise, we compared the original channel data acquired through the tissue with its estimated ballistic-wave component, as well as their corresponding spectra. We also compared performance of the proposed technique to F-X filter, which is a popular linear-prediction-based filter used to suppress noise in channel data. After the removal of acoustic noise from the channel data, coherence across the aperture increases. The average nearest-neighbor cross-correlation computed on the original data is 0.47, while the nearest-neighbor cross-correlation of the estimated ballistic-wave component is 0.81 or 0.97, depending whether the experimental or theoretical signal-PEFs are used in the estimation process.

1. INTRODUCTION

In medical ultrasound imaging, separating echoes due to multiple and off-axis scattering from the ballistic wavefronts of interest is needed in order to reduce the acoustic noise and improve visibility of tissue structures in a B-mode image.[1,2] Furthermore, estimating and suppressing such noisy echoes can increase coherence of signals across the aperture[3] and enable various phase-aberration-correction techniques and sound-speed estimators in heterogeneous media. The frequency-space (F-X) prediction filter has been shown to suppress random (white) noise in ultrasound data and enhance contrast of anechoic targets.[4] In the following, we use prediction-error filters (PEFs) to model the signal and the additive acoustic noise components of the individual-element data collected *ex vivo*. Following a pattern-based approach, the signal-PEF is first estimated from the noise-free data, and the noise-PEF is obtained by deconvolving the original (i.e. noisy) data with the signal-PEF. The two filters

Contact information: joseph29@sep.stanford.edu, marko.jakovljevic@stanford.edu, ettore88@sep.stanford.edu

Medical Imaging 2019: Ultrasonic Imaging and Tomography, edited by Brett C. Byram, Nicole V. Ruiter, Proc. of SPIE Vol. 10955, 109550R · © 2019 SPIE
CCC code: 1605-7422/19/$18 · doi: 10.1117/12.2513514

are then applied to separate the signal and noise components and increase the coherence of individual-element data. As another version of the method, we also estimate the signal-PEF from the VCZ theorem, which models echoes from the diffuse scatterers. This approach does not require direct noise-free measurements and could be applied to *in vivo* imaging.

2. METHODS

The individual element data was collected from a L12-3v linear array attached to a Verasonics Vantage 256 scanner. The transmit center-frequency was 7MHz. The data were acquired on a speckle generating phantom (Model 534, ATS, Norfolk, VA) through a 10mm layer of bovine tissue, and the pattern-based method was used to separate signal from the coherent noise in the acquired data.[5]

The pattern-based method for separating signal and coherent noise uses multidimensional non-stationary PEFs as part of a two-stage least-squares optimization to estimate the signal and noise. The method relies on three major assumptions. The first is that the signal and noise follow an additive model,

$$\mathbf{d} = \mathbf{s} + \mathbf{n} \tag{1}$$

where $\mathbf{d}$, $\mathbf{s}$ and $\mathbf{n}$ are vectors containing the recorded data, the signal, and the noise, respectively. Secondly, it is assumed that the spectra of the signal and noise are locally spatially uncorrelated. (i.e. they have different patterns). Because both the signal and noise in general will be coherent, this assumption will not always be valid, which might have an impact on the resulting signal estimate. Lastly, it is assumed that the signal and noise can be modeled via non-stationary multidimensional PEFs.[6] When estimating a prediction-error filter (PEF), we assume signals follow an autoregressive (AR) model

$$s(k) - a_1 s(k-1) - ... - a_M s(k-M) = n(k), \tag{2}$$

where $s(k)$ is the signal at sample k, $a_1, a_2, \ldots, a_M$ are the AR coefficients, M specifies the order of the autoregressive process, and n is white noise. In other words, the AR model allows the signal $s(k)$ to be expressed as a linear combination of M preceding samples in the sequence plus an error term (modeled as white noise). Considering that our discrete signal s is N samples in length, we can write out equation (2) for all N samples resulting in a system of $N-M$ equations with M unknowns. Provided that $M > N-M$, we can formulate the following regression that allows us to solve for the coefficients $\mathbf{a} = \begin{bmatrix} a_1 & \ldots & a_M \end{bmatrix}^T$

$$\mathbf{S}\mathbf{a} \approx \mathbf{s}, \tag{3}$$

where $\mathbf{S}$ is a matrix consisting of $N-M$ rows and M columns and contains all of the samples used to predict future samples (the elements of signal scaled by the elements of $\mathbf{a}$ in equation 2) and the vector $\mathbf{s}$ contains the $N-M$ future samples of the signal (the next sample we desire to predict). As the coefficients $\mathbf{a}$ are used to predict future samples of the signal $\mathbf{s}$, it is called a prediction filter. We can change it to a PEF by appending a unit coefficient to the beginning of $\mathbf{a}$

$$\mathbf{f} = \begin{bmatrix} 1 & -\mathbf{a} \end{bmatrix}^T. \tag{4}$$

To account for this additional coefficient, we create a matrix $\mathbf{D}$ that contains all of the coefficients $\mathbf{S}$ with $\mathbf{s}$ as an additional column. With this change, we can now express regression (3) as

$$\mathbf{D}\mathbf{f} \approx \mathbf{0}, \tag{5}$$

where $\mathbf{D}$ can be written in block form as $\mathbf{D} = \begin{bmatrix} \mathbf{s} & \mathbf{S} \end{bmatrix}$. Regressions (3) and (5) are mathematically equivalent, but state the idea in different ways: while regression (3) states that we desire to find filter coefficients that can optimally predict future samples of our signal, regression (5) states we desire to find a filter such that the prediction-error is zero. Upon estimating a PEF, the PEF has the very useful property of whitening the signal upon which it is estimated. This means that its coefficients contain the inverse spectrum (autocorrelation) of the signal. Additionally, while all of the previously-described theory considers stationary signals, for all of the examples in this work we estimate non-stationary PEFs that allow for a smoothly changing spectrum in the RF data along both the axial and lateral dimensions.

In the pattern-based method for separating coherent signal and noise, we estimate two PEFs, one for the signal $\mathbf{F}_s$ and one for the noise $\mathbf{F}_n$. The operators $\mathbf{F}_s$ and $\mathbf{F}_n$ are typically estimated using proxies of the signal and the noise. Herein, we acquired phantom data without tissue to use it as a signal proxy in order to estimate the coefficients $\mathbf{F}_s$. In order to estimate a proxy for the noise (denoted as $\hat{\mathbf{n}}$) we convolve the estimated signal-PEF with the data

$$\mathbf{F}_s\mathbf{d} = \mathbf{F}_s(\mathbf{s}+\mathbf{n}) = \hat{\mathbf{n}} \tag{6}$$

where we used equation (5) and the assumption that the signal and the noise are spatially uncorrelated. With the noise proxy available, a similar regression to that of equation (5) can be solved in order to obtain the noise PEF coefficients. Upon solving for the filter coefficients, we obtain non-stationary multidimensional PEFs that contain the approximate inverse spectra of the signal and noise.[7] The operators $\mathbf{F}_s$ and $\mathbf{F}_n$ are formed from the PEF coefficients and used as constraining terms in the following cost function, which is minimized to obtain the estimates of $\mathbf{s}$ and $\mathbf{n}$

$$J(\mathbf{s},\mathbf{n}) = \frac{1}{2}||\mathbf{s}+\mathbf{n}-\mathbf{d}||_2^2 + \frac{\epsilon_s^2}{2}||\mathbf{F}_s\mathbf{s}||_2^2 + \frac{\epsilon_n^2}{2}||\mathbf{F}_n\mathbf{n}||_2^2, \tag{7}$$

In equation (7), the two weighting coefficients ϵ_s and ϵ_n are empirically determined.

A different approach to obtain a signal proxy, which is employed to estimate the operator $\mathbf{F}_s$, is to use first principles to construct the autocorrelation of the proxy signal. In fact, the second-order statistics of the ultrasound signals received across the aperture can be modeled using the Van Cittert-Zernike (VCZ) theorem.[8] Mallart and Fink applied the VCZ theorem to pulse-echo ultrasound[8] and derived the expression for normalized covariance of the received pressure field when imaging diffuse scatterers. In such a scenario, the normalized covariance can be expressed as autocorrelation of the transmit aperture:

$$C'_{rf}(\Delta x) = \int_{-\infty}^{+\infty} TX(x+\Delta x)\,TX(x)dx, \quad -D < \Delta x < D \tag{8}$$

where TX is the transmit apodization function and D is the length of the aperture. When using uniform (i.e. rectangular) apodization, the normalized covariance of received pressure field becomes a triangle function with base $2D$. It is worth noting that these results are valid only when the observation points in aperture data (x_1 and x_2) are located on the focused surface,[8] meaning that geometric delays are usually applied to received signals before estimating $C_{rf}(\Delta x)$. By using equation (8) we can estimate the proxy response of the signal necessary to estimate the operator $\mathbf{F}_s$ without having recorded ideal radio-frequency ballistic echos, but directly from first principles.

3. RESULTS AND DISCUSSION

Figures 1, 2 and 3 show information obtained from the individual element signals acquired from the speckle phantom through a layer of tissue. Figure 1 shows the original (i.e., unfiltered) radio-frequency (RF) traces, along with the F-X filtered signal and the PEF-based estimates of signal and noise. The noise-free phantom data (acquired without the tissue) was used to compute the PEF operator for the signal F_s in equation (7). In all images, traces have been delayed to account for geometric-path differences, assuming the speed of sound of 1540 m/s. In the original data, wavefronts due to reverberation and off-axis scattering are visible and they corrupt the phantom signal (recorded beyond 10 mm depth). F-X filter suppresses the random noise, but the structured noise can still be observed through depth. The PEF-estimate of signal contains mainly ballistic wavefronts, while PEF-estimate of the noise contains wavefronts from multiple and off-axis scattering; this shows that the signal and noise components have been successfully separated using PEFs. As the noise is removed, coherence of the signals across the aperture increases, with the average nearest-neighbor cross-correlation measured at 0.47 for the unfiltered element traces and 0.81 for the PEF-estimate of signal.

2-D frequency spectra of the filtered and unfiltered element traces are displayed in Figure 2. All spectra are computed from the traces windowed to eliminate the signal from top 10 mm (where the tissue is located). F-X filtering removes some of the broadband noise present in the original data, but a narrow-band, low-axial-frequency component indicative of structured noise remains in the spectrum. The pattern-based approach removes this

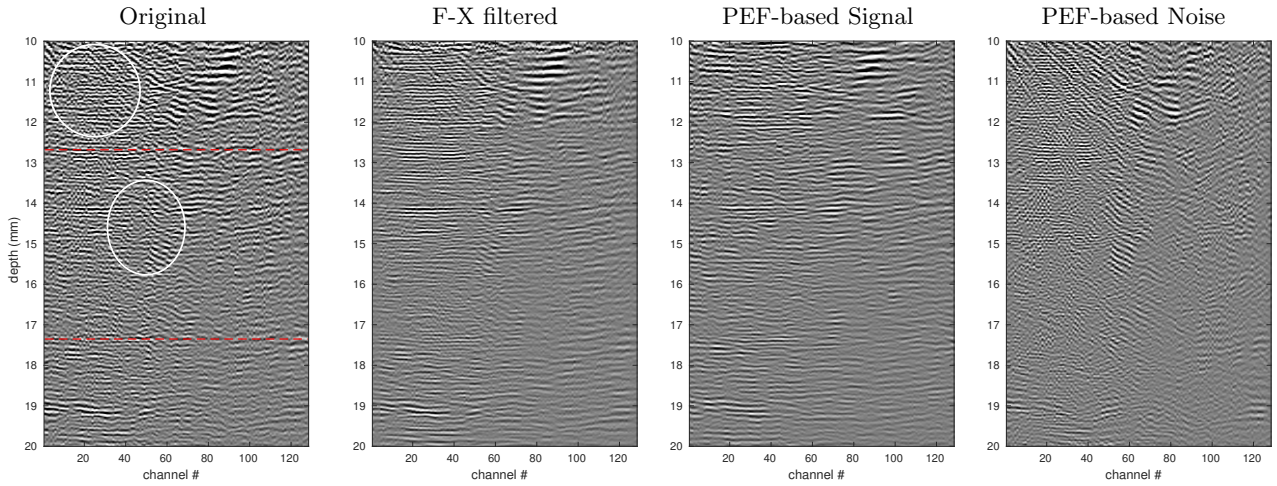

Figure 1. Radio-frequency signals received on the individual transducer elements from a speckle region of the phantom and through a 10 mm thick layer of beef tissue. The original (unfiltered) data (a), F-X filtered data (b), speckle signal estimated from the data following the pattern-based approach (c), and noise component of the data estimated with the pattern-based approach (d). In (b), the random noise is suppressed, but wavefronts from multiple and off-axis scattering can still be observed through depth. In (c), the estimated signal component contains mainly ballistic wavefronts, while multiples are removed and estimated as a part of the noise component in (d). Examples of multiples that are removed from the original data and estimated as part of noise are circled in (a). Range of depths used to compute the nearest-neighbor cross-correlation is denoted using dashed red lines.

narrow-band noise from the signal and groups it into the noise spectrum. The estimated signal spectrum is dominated by low lateral frequencies, as expected for the uniform speckle target.

Figure 3 shows the PEF-estimates of signal and noise when the VCZ theorem is used to compute the PEF operator for signal $\mathbf{F}_s$ in equation (7). The estimated signal component contains less broadband noise than the signal estimate in Figures 1 and 2 implying that the VCZ theorem gives a better proxy of the desired signal than the direct phantom measurements. This observation is supported by an increase in the nearest-neighbour cross-correlation; when using the theory-derived signal-PEF it is measured at 0.97. The above described behavior is due to the fact that the no-tissue phantom measurements are still corrupted by electronic noise of the imaging system and the estimated operator $\mathbf{F}_s$ then models some of this noisy energy in addition to the signal (i.e., there is overfitting). The estimate of the noise using the VCZ theorem contains both broadband and narrowband energy of the noisy component (Figure 3d).

Figure 4 shows the average coherence measured across the aperture for the unfiltered and filtered channel signals as well as for the estimated noise component. After applying the proposed filtering method, the separated signal shows higher coherency for greater lag values compared to the original recorded data. This figure allows us to quantitatively evaluate the efficacy of the filtering technique. In addition, as expected, the coherency of the estimated noise drastically decreases even for low lag values.

4. CONCLUSIONS

While the linear prediction filtering has been applied before to remove the random (white) noise from the ultrasound data, we use the non-stationary PEFs to estimate both the signal and the additive structured noise such as multiples and off-axis wavefronts. The proposed algorithm is tested on phantom data corrupted with clutter from a 10 mm thick layer of beef tissue. Comparison of the estimated signal and noise spectra shows the ability of the proposed technique to successfully separate different data components when their spectral properties locally differ. We also explored the use of an autocorrelation function of speckle based on the VCZ theorem to estimate the signal PEF used as a part of the proposed filtering method. This approach achieved

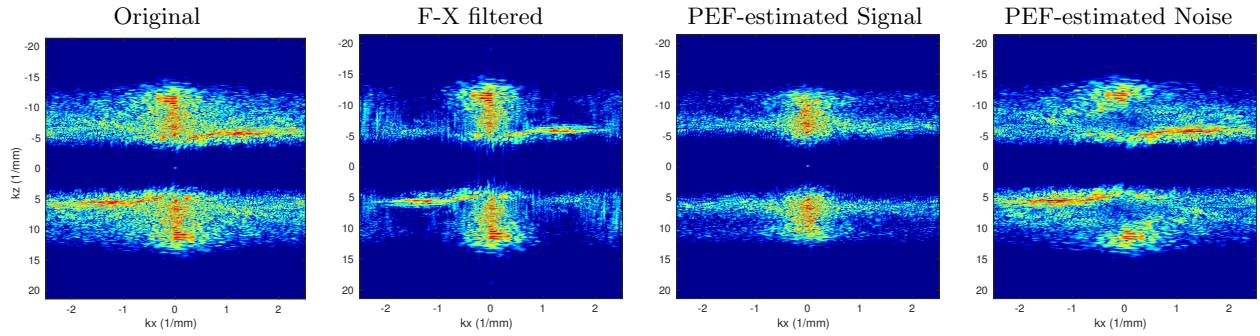

Figure 2. 2-D spectra of the individual element signals presented in Figure 1. Spectrum of the unfiltered data (a), spectrum of the F-X filtered data (b), spectrum of the signal component estimated with the pattern-based approach (c), and spectrum of the noise component estimated with the pattern-based approach (d). The element data used to compute the spectra was windowed to eliminate the top 10 mm where the tissue lies. In (b), F-X filtering removes some of the broadband noise present in the original data, but the narrow-band components that correspond to the structured acoustic noise remain. Pattern-based approach separates these narrow-band components from the signal, and they can be observed in the noise spectrum in (d). The estimated signal spectrum in (c) is dominated by low lateral frequencies, as expected for the uniform speckle target. All the spectra are normalized with their respective maxima and displayed over 30 db dynamic range.

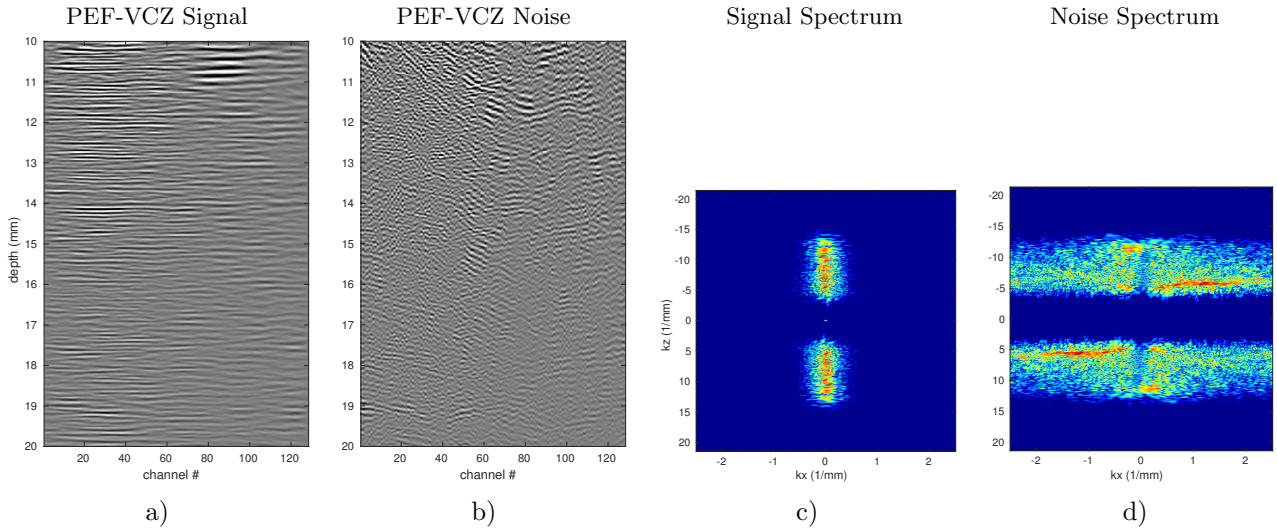

Figure 3. PEF-estimates of signal and noise when the VCZ theorem is used to compute the PEF operator for signal $\mathbf{F}_s$ in equation (7). Individual element traces containing estimated signal (a), element traces containing estimated noise (b), 2-D signal spectrum (c), 2-D noise spectrum (d). The signal spectrum shows less broadband content compared to Figure 2 indicating that the VCZ theorem is a better proxy of the desired signal than a direct phantom measurement. The corresponding estimate of the noise contains both broadband and narrowband noise components.

better signal-noise separation compared to the phantom-based filtering technique. This extension of the method could be also used to deconvolve *in vivo* data and find the PEF associated to the noise.

ACKNOWLEDGMENTS

This work is supported by NIH grant R01-EB013661-05. The authors also wish to thank Dongwoon Hyun for kindly sharing the phantom data. The authors would also like to thank Rehman Ali for useful discussions and insights on the topic.

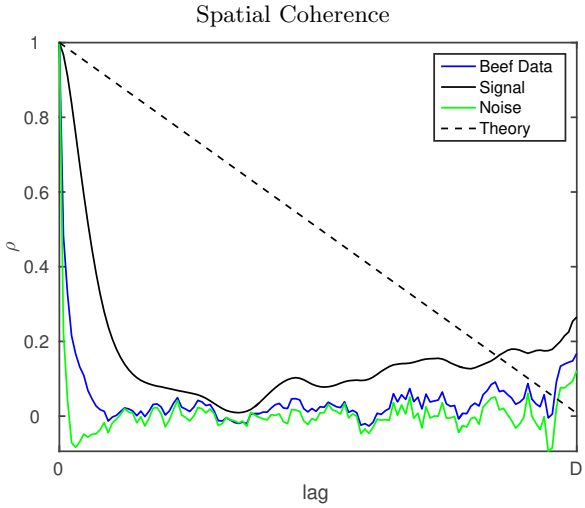

Figure 4. Average spatial coherence measured across the filtered and unfiltered element signals captured through a layer of beef tissue. The spatial coherence measured on the unfiltered data is denoted as "beef", while the PEF-estimated signal and noise components are denoted as "signal" and "noise", respectively. The estimated signal component shows increased coherence across the aperture compared to the original data, especially around the region of short lags. The signal and noise estimates were computed using the VCZ theorem to model the PEF-signal operator F_s. All coherence curves were computed over the 5 mm region of data centered around the focal depth. Theoretical coherence of the noise-free speckle signal (as predicted by the VCZ theorem) is provided as a reference and is denoted with a black dashed line.

REFERENCES

[1] Lediju, M., Pihl, M. J., Dahl, J. J., and Trahey, G. E., "Quantitative assessment of the magnitude, impact, and spatial extent of ultrasonic clutter," *Ultrasonic Imaging* **30**(3), 151–168 (2008).

[2] Byram, B., Dei, K., Tierney, J., and Dumont, D., "A model and regularization scheme for ultrasonic beamforming clutter reduction," *IEEE TUFFC* **62**(11), 1913–1927 (2015).

[3] Pinton, G. F., Trahey, G. E., and Dahl, J. J., "Spatial coherence in human tissue: Implications for imaging and measurement," *IEEE TUFFC* **61**(12), 1976–1987 (2014).

[4] Shin, J. and Huang, L., "Spatial prediction filtering of acoustic clutter and random noise in medical ultrasound imaging," *IEEE Transactions on Medical Imaging* **36**(2), 396–406 (2017).

[5] Guitton, A., "Multiple attenuation in complex geology with a pattern-based approach," *Geophysics* **70**(4), V97–V107 (2005).

[6] Fomel, S., "Adaptive multiple subtraction using regularized nonstationary regression," *Geophysics* **74**(1), V25–V33 (2008).

[7] Claerbout, J. F. and Fomel, S., [*Geophysical image estimation by example*], Citeseer (2008).

[8] Mallart, R. and Fink, M., "The van Cittert-Zernike theorem in pulse echo measurements," *Journal of Acoustical Society of America* **90**(5), 2718–2727 (1991).